



**UNIVERSITY OF LEEDS**

This is a repository copy of *Sensitive and selective Affimer-functionalised interdigitated electrode-based capacitive biosensor for Her4 protein tumour biomarker detection*.

White Rose Research Online URL for this paper:  
<http://eprints.whiterose.ac.uk/127708/>

Version: Accepted Version

---

**Article:**

Zhurauski, P, Arya, SK, Jolly, P et al. (4 more authors) (2018) Sensitive and selective Affimer-functionalised interdigitated electrode-based capacitive biosensor for Her4 protein tumour biomarker detection. *Biosensors and Bioelectronics*, 108. pp. 1-8. ISSN 0956-5663

<https://doi.org/10.1016/j.bios.2018.02.041>

---

© 2018 Elsevier B.V. This manuscript version is made available under the CC-BY-NC-ND 4.0 license <http://creativecommons.org/licenses/by-nc-nd/4.0/>

**Reuse**

This article is distributed under the terms of the Creative Commons Attribution-NonCommercial-NoDerivs (CC BY-NC-ND) licence. This licence only allows you to download this work and share it with others as long as you credit the authors, but you can't change the article in any way or use it commercially. More information and the full terms of the licence here: <https://creativecommons.org/licenses/>

**Takedown**

If you consider content in White Rose Research Online to be in breach of UK law, please notify us by emailing [eprints@whiterose.ac.uk](mailto:eprints@whiterose.ac.uk) including the URL of the record and the reason for the withdrawal request.



[eprints@whiterose.ac.uk](mailto:eprints@whiterose.ac.uk)  
<https://eprints.whiterose.ac.uk/>

# **Sensitive and selective Affimer-functionalised interdigitated electrode-based capacitive biosensor for Her4 protein tumour biomarker detection**

Pavel Zhuravski<sup>1,a</sup>, Sunil K. Arya<sup>1,b,\*</sup>, Pawan Jolly<sup>1,c</sup>, Christian Tiede<sup>2</sup>, Darren C. Tomlinson<sup>2</sup>,

Paul Ko Ferrigno<sup>3</sup>, Pedro Estrela<sup>1,\*</sup>

<sup>1</sup> Department of Electronic and Electrical Engineering, University of Bath, Bath BA2 7AY, United Kingdom

<sup>2</sup> Astbury Centre for Structural and Molecular Biology, University of Leeds, Leeds LS2 9JT, United Kingdom

<sup>3</sup> Avacta Life Sciences Ltd, Unit 20, Ash Way, Thorp Arch Estate, Wetherby LS23 7FA, United Kingdom

\*Corresponding authors: Phone: +44 7405106621, Email: [sunilarya333@gmail.com](mailto:sunilarya333@gmail.com) (Sunil K Arya), [P.Estrela@bath.ac.uk](mailto:P.Estrela@bath.ac.uk) (Pedro Estrela)

<sup>a</sup> Current address: Zimmer & Peacock Ltd, 1 Market Hill, Royston SG8 9JL, United Kingdom

<sup>b</sup> Current address: Gwent Electronic Materials Ltd, Monmouth House, Mamhilad Park, Pontypool, Torfaen NP4 0HZ, United Kingdom

<sup>c</sup> Current address: Wyss Institute for Biologically Inspired Engineering, Harvard University, Boston, MA 02115, USA

## **Abstract**

A novel Affimer-functionalised interdigitated electrode-based capacitive biosensor platform was developed for detection and estimation of Her4, a protein tumour biomarker, in undiluted serum. An anti-Her4 Affimer with a C-terminal cysteine was used to create the bio-recognition layer via self-assembly on gold interdigitated electrodes for the sensor fabrication. Electrochemical impedance spectroscopy (EIS) in the absence of redox markers was used to evaluate the sensor performance by monitoring the changes in capacitance. The Affimer sensor in buffer and in undiluted serum demonstrated high sensitivity with a broad dynamic range from 1 pM to 100 nM and a limit of detection lower than 1 pM both in buffer and in serum. Furthermore, the Affimer sensor demonstrated excellent specificity with negligible interference from serum proteins, suggesting resilience to non-specific binding. The sensing ability of the present Affimer sensor in spiked undiluted serum suggests its potential for a new range of Affimer-based sensors. The

fabricated Affimer sensor can thus be further adapted with other probes having affinities to other biomarkers for a new range of biosensors.

---

**Keywords:** Affimer; impedimetric; capacitance; biosensor; serum; Her4

## 1. Introduction.

In recent years, the development of novel bioreceptors has rapidly expanded. The primary motivations behind these developments for the biochemists / molecular biologists have been not only the large biological potential but also an enormous demand for synthetic bio-receptors. Whilst antibodies remain the workhorse choice for the molecular recognition for many biosensing devices and laboratory assays, their usage can still impose limitations on technology adoption, in particular due to their large size, multi domain protein structure with unstable disulphide bond, instability during regeneration, unpredictable interaction with target, along with difficulty in production and high cost (Raina et al. 2015; Song et al. 2008; Vazquez-Lombardi et al. 2015). One long-championed alternative to antibodies has been DNA aptamers, which are single stranded oligonucleotide sequences possessing high affinity and specificity for its desired target. DNA aptamers, in their own right, have been extensively used for biosensing applications ('aptasensors'), yet the approach has had little impact as a viable bioanalytical tool to date (Rimmele 2003; Xu et al. 2009). Despite many advantages over antibodies, they still possess a number of limitations, for example, degradation by nucleases (DNAse and RNAse) or protein fouling in serum due to DNA binding proteins (Keum and Bermudez 2009; Sylvia et al. 1975).

A new emerging class of bioreceptors inspired from the increasing understanding of antibodies are Affimers<sup>®</sup>, generically termed as peptide aptamers (Tiede et al. 2017; Woodman et al. 2005). Based on their scaffold origin from human stefin A protein or consensus plant phytocystatin protein, Affimers are classified as type I and type II (Tiede et al. 2014) with both types containing an  $\alpha$ -helix and four  $\beta$ -sheets (Bedford et al. 2017). Affimers are small receptor non-antibody proteins (Mw ~ 15 kDa, size 2-4 nm) mainly containing two 9 amino acids variable regions for molecular recognition and function as a protein platform for the restriction of two variable recognition peptide regions (Bedford et al. 2017; Johnson et al. 2012; Raina et al. 2015; Straw et al. 2013; Tiede et al. 2014; Tiede et al. 2017; Woodman et al. 2005). Furthermore, Affimers mimic the molecular recognition characteristic of monoclonal antibodies for the detection

of biomolecules. Unlike antibodies, Affimers display robust characteristics of low molecular weight, high thermostability, and resistance to extreme pH conditions, ease of site specific functionalization, low production cost with high reproducibly using E. coli recombinant protein expression systems (Arrata et al. 2017; Bedford et al. 2017; Koutsoumpeli et al. 2017; Kyle et al. 2015; Raina et al. 2015; Rawlings et al. 2015; Tiede et al. 2014; Vazquez-Lombardi et al. 2015; Wang et al. 2017b). Of key relevance, there is recent work demonstrating the application of Affimers for biosensing applications (Estrela et al. 2010; Ko Ferrigno 2016; Koutsoumpeli et al. 2017; Raina et al. 2015; Sharma et al. 2016; Wang et al. 2017b).

This study aims to develop for the first time an Affimer-based electrochemical sensor targeting Her4. Her4 belongs to the HER (human epidermal growth factor receptor related) family, which includes four transmembrane receptors tyrosine kinase (RTKs) named EGFR: Her1 (ErbB1), Her2 (ErbB2), Her3 (ErbB3) and Her4 (ErbB4) (Tebbutt et al. 2013). The altered expression of the HER family have been implicated in many human diseases and has been proposed as a potential prognostic and diagnostic biomarker (Zhao et al. 2014). Her4, for example, is a ~70 kDa protein and an emerging biomarker for the detection of gastrointestinal stromal tumours, which accounts for more than 80% of all gastrointestinal mesenchymal tumours and is the most common type of gastrointestinal tumours with increased incidence rate (Mucciarini et al. 2007; Nilsson et al. 2005; Sandvik et al. 2011; Steigen and Eide, 2009). In addition, the Her4 ectodomain has been detected at low concentrations in the serum of breast cancer patients and could potentially serve as a prognostic or predictive marker as part of a profile with other biomarkers (Hollmén et al. 2012; Olsen et al. 2009).

Recently the use of electrochemical biosensors for biomarker detection has gained much attention. Among various biosensors, electrochemical impedance spectroscopy (EIS)-based sensing for probing the features of surface-modified electrodes has recently gained particular attention for label free, fast, sensitive and miniaturized biosensor development (Arya et al. 2014; Arya et al. 2018; Gong et al. 2017; Sharma et al. 2016). An EIS measurement uses a small amplitude

perturbing sinusoidal alternative voltage signal applied during scanning over a wide range of frequencies in an electrochemical cell to measure the resulting AC current response. EIS exploits resistive and capacitive properties of material for analysis. Using proper equivalent circuit models, EIS can be utilized for the characterization, analysis and study of coatings, fuel cells batteries, corrosion phenomena, electrode kinetics, conducting polymers, semiconductors, sensors, animal and plant tissues and general material (Guan et al. 2004; Katz and Willner 2003). EIS-based biosensors measure changes in impedance or capacitance that occur at an electrode surface upon target binding and can be utilized for wide concentration range estimation (Ramón-Azcón et al. 2008). Using EIS researchers have reported measurement of various small and large size targets such as cortisol in saliva, epidermal growth factor receptor (EGFR), cardiac troponin I, tau protein, C-reactive protein in blood, insulin in blood serum, etc in wide concentration ranges from low picomolar to high nanomolar (Bryan et al. 2013; Pasha et al. 2014; Vasudev et al. 2013; Wang et al. 2016; Wang et al. 2017a; Xu et al. 2013). In these and other reports researchers have shown sensitive measurements of targets in real samples using EIS either directly or after washing the electrode. Furthermore, recently it has been shown that the development of EIS-based biosensor using interdigitated microelectrodes (ID $\mu$ Es) can provide added advantages of superior sensitivity, faster steady state, better reaction kinetics, and better signal-to-noise ratio (Arya and Bhansali 2012; Ramón-Azcón et al. 2008; Varshney and Li 2009). Also, EIS-based biosensor development provides options of measurement of impedance/charge transfer resistance in Faradaic mode using redox markers in solution (Arya et al. 2014; Santos et al. 2014) or capacitance in non-Faradaic mode without any redox markers (Berggren et al. 2001; Luo and Davis 2013; Qureshi et al. 2010) for highly sensitive detection of analytes. Non-Faradaic approaches do not require the presence of redox probes in the analytical solution; they measure capacitive changes occurring due to bio recognition causing charge distribution, surface dielectric properties or local conductance variations via water molecules displacement and ions movement away from the surface during molecular interactions. In non-Faradaic mode, no redox probes need to be introduced to the sample to be

measured; hence it is a method with direct applicability for point-of-care diagnostics (Arya et al. 2018; Berggren et al. 2001; Luo and Davis 2013; Qureshi et al. 2010).

This study aims to utilize the advantage of Affimer combined with non-Faradaic impedance and ID $\mu$ E to develop, for the first time, an Affimer-based electrochemical biosensor for Her4 detection in undiluted serum. For biosensor development, gold ID $\mu$ E chips were functionalized with cysteine modified Her4 Affimer via self-assembly and used for specific capture of Her4 protein. The surface was further blocked using phosphate buffer saline-tween 20 based starting block (SB) to prevent non-specific binding and fouling of the surface. Non-Faradaic electrochemical impedance spectroscopy was utilized to quantify Her4 binding events in buffer and serum samples by monitoring the changes in capacitance. The fabricated Affimer biosensor demonstrated excellent sensitivity and a wide dynamic range from 1 pM to 100 nM in both buffer and spiked undiluted human serum samples. When challenged with other serum proteins, the Affimer exhibited excellent specificity towards Her4. The present Affimer biosensor exhibits with its low background and broad linear response range, will pave the way to new platforms for alternative low cost and rapid multiplexed biosensors.

## **2. Experimental**

### **2.1. Reagents**

Cysteine terminated Affimer binders to Her4 have previously been characterised in affinity staining cells and in super-resolution microscopy (Tiede et al. 2017). The Affimer demonstrated excellent specificity for imaging of fixed cell and single-particle tracking on live cells. For binding studies, different concentrations of Her4 and control molecules were prepared in 10 mM phosphate buffer saline (PBS), pH 7.4 or in undiluted serum. PBS-Tween20 (PBST20) based starting block (SB) was procured from Fisher Scientific (UK); Dulbecco's Phosphate Buffered Saline and Phosphate Buffered Saline with 0.05% Tween20 was procured from Sigma (UK). For serum spiking studies to mimic clinical samples, human serum, from human male AB was procured from

Sigma. All other chemicals were of analytical grade and were used without further purification. All aqueous solutions were prepared using 18.2 M $\Omega$  cm ultra-pure water with a Pyrogard® filter (Millipore, MA, USA).

## 2.2. Apparatus

Biosensor fabrication was characterised using electrochemical impedance spectroscopy (EIS) in a three-electrode configuration with gold as counter and pseudo reference electrode at equilibrium potential (open circuit potential generated between electrodes dipped in electrolyte), without external biasing in the frequency range of 100 kHz - 100 mHz, with a 25 mV amplitude using a using a  $\mu$ Autolab III / FRA2 potentiostat/galvanostat (Metrohm, Netherlands). EIS measurements were carried out using 50  $\mu$ L of PBS solution (10 mM, pH 7.4) containing a mixture of 5 mM Fe(CN) $_6^{4-}$  (ferrocyanide) and 5 mM of Fe(CN) $_6^{3-}$  (ferricyanide) as a redox probe. For Her4 detection and estimation, non-Faradaic EIS measurements (absence of redox couple) were performed in a two interdigitated electrodes configuration in 10 mM PBS (pH7.4) in a frequency range 100 kHz - 100 mHz, with a 200 mV amplitude.

Surface characterisation of gold electrodes modified with Affimer was performed using EIS, surface plasmon resonance (SPR), contact angle and atomic force microscopy (AFM). Ambient contact mode (tapping mode) AFM imaging was performed using MultiMode NanoScope with IIIa controller (Bruker, Germany) in conjunction with version 6 control software. Gold chips modified as described in the fabrication section for gold electrodes were imaged with a 10 nm diameter AFM ContAl-G tip (BudgetSensors®, Bulgaria), images were then processed by the NanoScope Analysis software, version 1.5. Contact angle measurements were performed using an in-house built optical angle measurement system (Miodek et al. 2015). The electrodes were placed on the stage and a 5  $\mu$ L drop was dispensed on the electrode with the dispensing system. The wetting of surface was then captured using a Nikon p520 camera. Contact angle was measured using a screen protractor version 4.0 procured from Iconico. SPR measurements were performed using a Reichert SPR

7000DC (USA) dual channel flow spectrometer at 25 °C. 50 nm gold coated SPR gold chips, supplied from Reichert Technologies were used for studying the reaction on SPR. Prior to their modification, the chips were cleaned using piranha solution (3:1 H<sub>2</sub>SO<sub>4</sub>:H<sub>2</sub>O<sub>2</sub>) for 20 seconds and rinsed thoroughly with MilliQ water and dried using nitrogen gas. All buffers were filtered through 0.2 µm filters and degassed for 2 h by sonication prior to the experiment.

### **2.3. Electrode preparation and functionalisation**

#### 2.3.1 Gold electrode fabrication

Gold interdigitated micro-electrode arrays (IDµE) on silicon/silicon oxide wafers were created using lithographic and micro-fabrication techniques as described in an earlier report (Pui et al. 2013). In brief, Ti/Au (15 nm/200 nm) IDµE having fingers of 5 µm width and 3200 µm length, spaced at 10 µm and spread over a 5500 µm length were deposited on silicon/silicon oxide wafers using standard photolithography techniques. IDµE, reference and counter electrodes were patterned via photoresist spin coating followed by photolithography through a chrome mask and development. After the metal deposition an electron-beam evaporator, etching of unpatterned metal regions with Au etchant and Ti etchant was performed. Photoresist was then stripped in solvent followed by wafer cleaning and dicing. The schematics in Figure 1 summarize the electrode fabrication process along with an optical image of the chip showing the IDµE section.

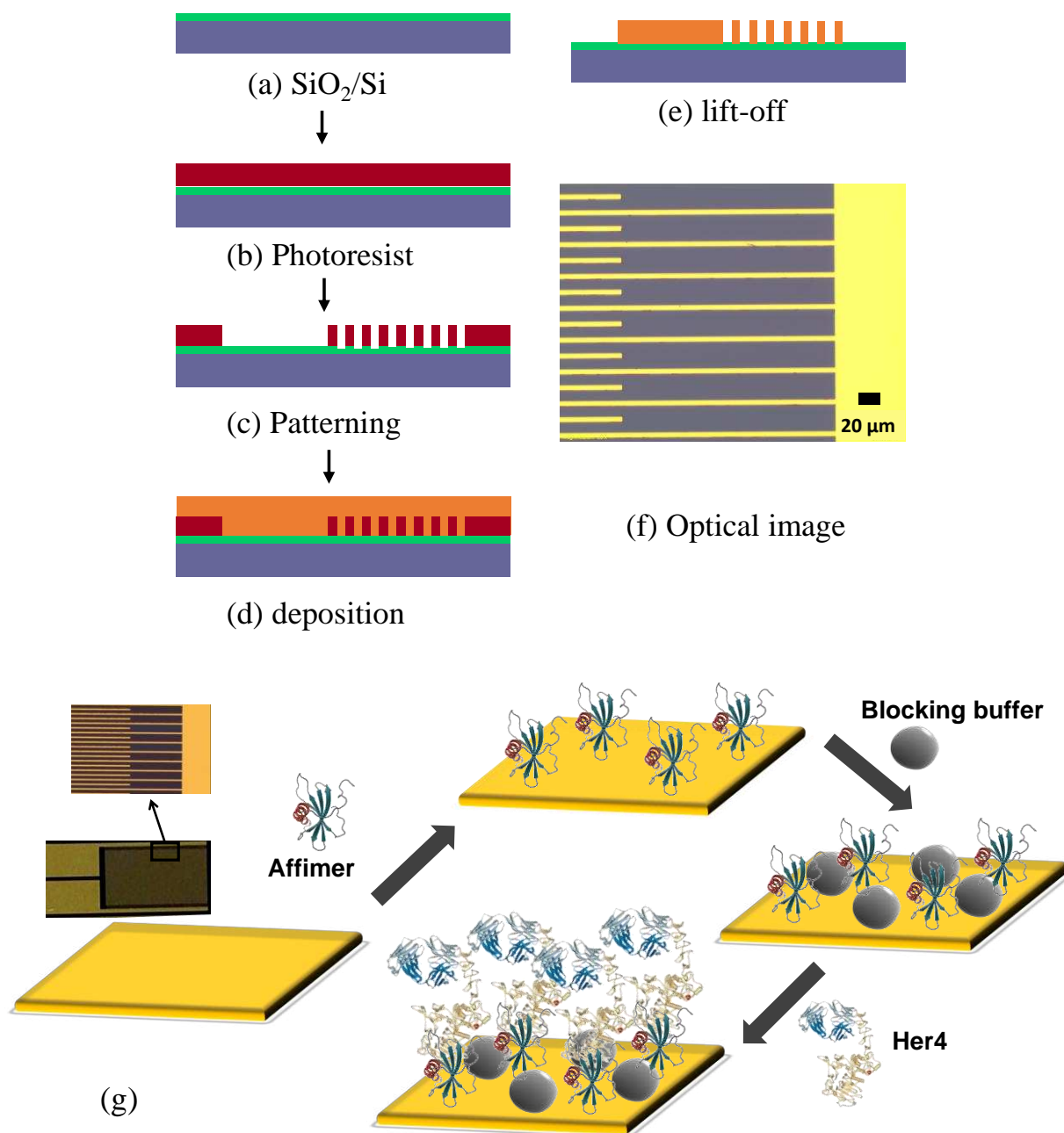


**Figure 1.** (a-e) Electrode fabrication process; (f) Optical image of chip showing IDμE section; (g) Schematic for Affimer sensor preparation and Her4 capture.

### 2.3.2 Gold electrode functionalization with Affimer

Prior to functionalisation, electrodes were pre-cleaned thoroughly with isopropyl alcohol, acetone and de-ionised milli-Q water (Millipore, UK), followed by 30 min treatment using UV-ozone (ProCleaner, BioForce Nanosciences, USA). For Affimer self-assembled monolayer (SAM) formation conditions were optimized and using optimized conditions 100 μg/mL solution of cys-

Her4 Affimer containing 5 mM Tris (2-carboxyethyl) phosphine hydrochloride (TCEP) was prepared in 10 mM PBS buffer (pH 7.4) and incubated for 30 min at 37 °C to reduce any disulphide bonds. After reduction, 50 µL of this mixture was poured onto the IDµE electrodes and incubated for 120 min at 37 °C. Thereafter, the chips were washed with PBST20 (10 mM, pH 7.4) and PBS (10 mM, pH 7.4) to remove any unbound Affimer. The chips were finally blocked with SB for 30 min and after removing extra solution, chips were stored at 4 °C till further use. Figure 1g shows the schematic for Affimer sensor electrode preparation.

### **3. Results and Discussion**

#### **3.1. Characterisation of the Affimer sensor fabrication**

##### **3.1.1 Contact angle and atomic force microscopic characterisation**

Contact angle and atomic force microscopy (AFM) were used to determine the efficiency of the Affimer immobilization onto the electrode surface. The effect of Affimer monolayer formation on the surface's hydrophilic/hydrophobic properties was estimated using contact angle images recorded on gold chips without any pattern. To measure contact angle, electrodes without and with Affimer monolayer were placed on the stage and a 5 µL of ultra-pure water drop was dispensed on the electrode. From Figure 2a, it is clear that clean gold showed a hydrophilic character with a contact angle value of 23°. After Affimer monolayer formation, the contact angle was found to increase to 44° (Figure 2b), confirming the immobilization of the Affimer. Increasing contact angle indicates a more hydrophobic character of the Affimer electrode as compared to gold. On the AFM studies, the images of blank gold and Affimer-modified gold surface presented in Figure 3 further confirm the Affimer binding. The Affimer modified surface showed more uniform morphology when compared with blank.

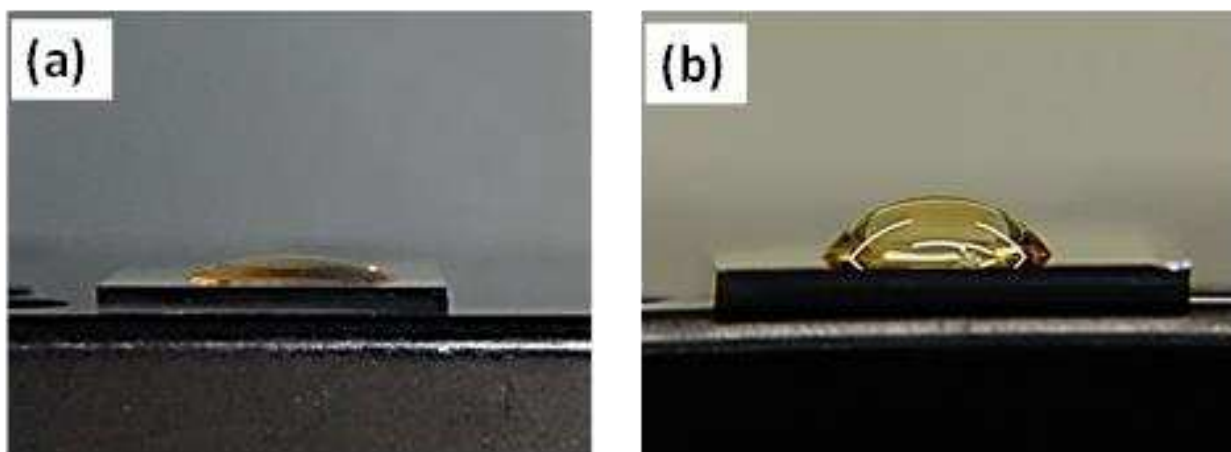


**Figure 2.** Contact angle images for (a) blank cleaned gold surface and (b) after Affimer SAM formation.

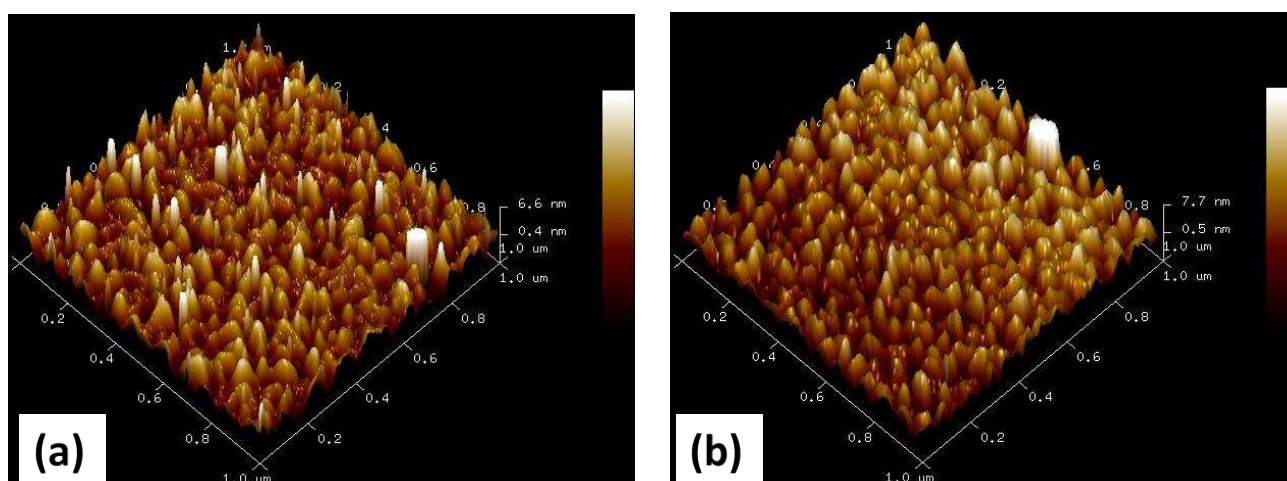


**Figure 3.** AFM images for (a) blank cleaned gold surface and (b) after Affimer SAM formation.

### 3.1.2. Electrochemical impedance spectroscopy and surface plasmon resonance characterisation

Faradaic-mode electrochemical impedance spectroscopy was utilised to further determine whether the Affimer has been immobilised on the surface (see Nyquist plots in Figure 4a). The plots follow a standard Randles equivalent circuit, as shown in Figure 4b (i), with the capacitance replaced by a constant phase element. After Affimer immobilization, the low frequency Warburg element is no longer observed and the plot resembles the equivalent circuit in Figure 4b (ii). The observed tail in low frequency region due to Warburg impedance in blank electrode spectra indicate

high conductivity of blank electrode, thus causing charge diffusion at lower frequency region. Whereas after Affimer binding surface become insulating due to immobilization of insulating protein of the surface, thus allowing no free diffusion of charge in lower frequency region and following circuit (ii). A change in charge transfer resistance ( $R_{ct}$ ) value from 680  $\Omega$  for blank to 50.7 k $\Omega$  for the Affimer SAM and blocker modified sensor surface shows the immobilisation of Affimer in high density forming SAM (Figure 4a). The large change in  $R_{ct}$  can be attributed to the insulating nature and dense immobilisation of pre-reduced Affimer solution onto the gold surface. For the observed high  $R_{ct}$  and assuming the measured current is mainly due to defects in the monolayer, the surface coverage was estimated using  $\theta = 1 - R_{ct}/R_{ct}^0$ , where  $R_{ct}$  and  $R_{ct}^0$  indicate the charge transfer resistance before and after monolayer formation, and found to be 98.66% coverage. It should be noted that high density immobilization of the capture molecules may not always result in better analyte capture probabilities and steric crowding effects of tightly packed receptor molecules may actually degrade the sensor performance (Bonanno and DeLouise 2007). To study this effect for Her4 Affimer, Affimer monolayer formation during optimization was also tested without pre-reduction and much lower impedance for immobilization was observed indicating porous film, however negligible response was observed in capacitive sensing for Her4 indicated necessary pre-reduction. Thus, pre-reduction was optimized and the best response was observed with Affimer monolayer formation after pre-reduction done via 30 min incubation of Affimer-TCEP mixture at 37 °C to reduce any disulphide bonds. A very small change in impedance is observed after the blocking step, further suggesting the dense coverage by Affimer, which leave very few free spaces on the surface to be taken up by blocker protein molecules.

To confirm the immobilization and ability of surface attached Affimer molecules to capture Her4 molecules, SPR spectra was recorded. For SPR studies, gold chips were modified using the same procedure as that used for ID $\mu$ E modification. The modified SPR chips were then utilised to investigate Her4 capture in PBST20, i.e. in the same buffer as used for the impedance sensor. In Figure 4c increase in SPR signal after introduction of Affimer solution and a large change in the

signal indicate successful binding of Affimer. Further an increasing SPR signal for increasing Her4 concentration in Figure 4d, confirms the activity of Affimer molecules bound on surface, in particular above ~100 pM of Her4.

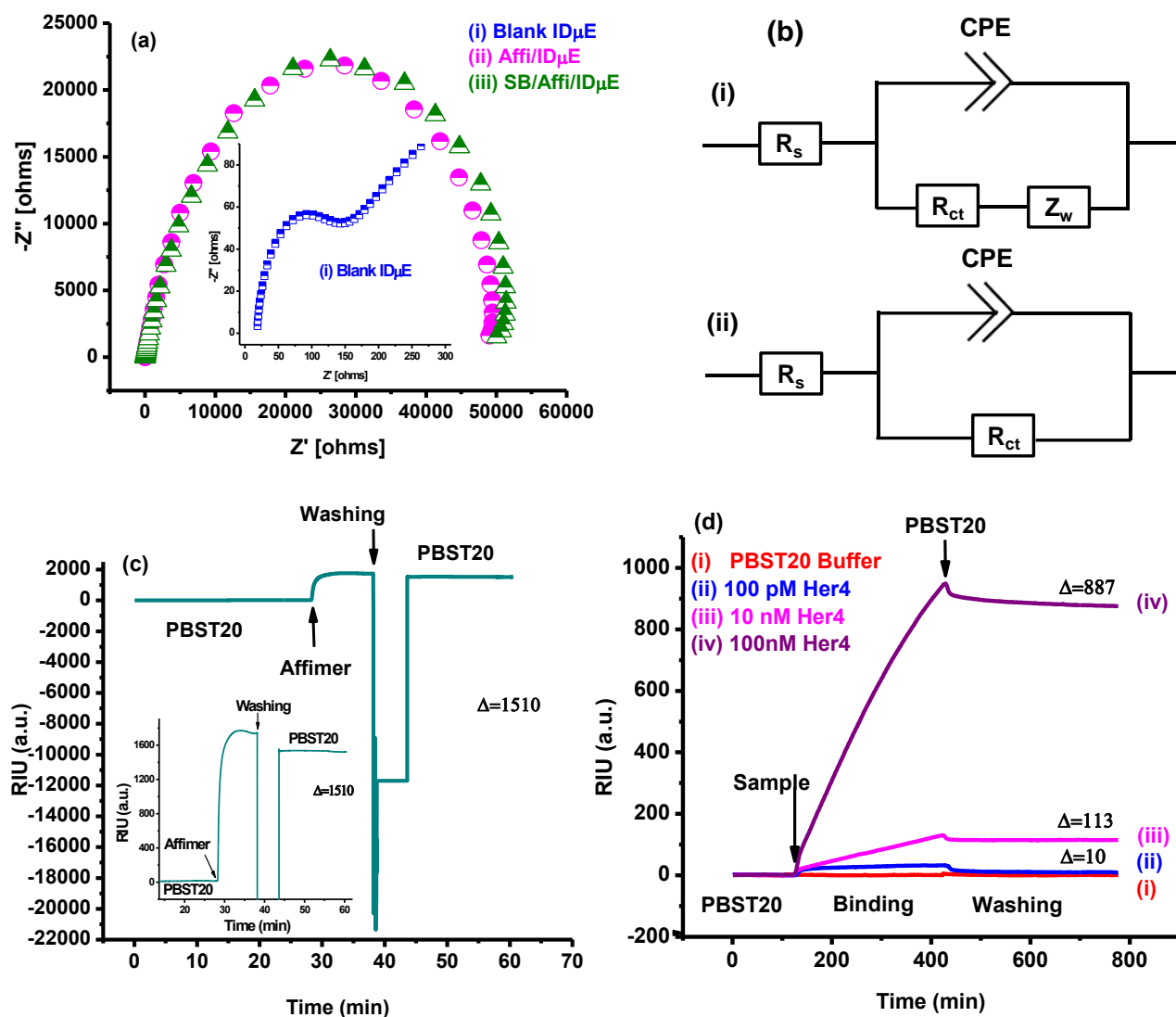


**Figure 4.** (a) Nyquist plots for (i) blank ID $\mu$ E, (ii) Affimer/ID $\mu$ E and (iii) blocker/Affimer/ID $\mu$ E. (b) Equivalent circuits used for EIS fitting. (c) Real time SPR spectra for Affimer immobilization. (d) Real time SPR response for (i) PBST20, (ii) 100 pM Her4 in PBST20, (iii) 10 nM Her4 in PBST20 and (iv) 100 nM Her4 in PBST20 using Affimer sensor.

### 3.2. Her4 studies

#### 3.2.1 Capacitive measurement via electrochemical impedance for Her4 in PBS

The SB/Affimer/ID $\mu$ E based sensors were used to investigate the interaction between surface bound Affimer and Her4 concentrations from 1 pM to 100 nM (Figure 5). For measurement of each concentration, the bio-electrode was incubated with a Her4 solution for 30 min, followed by PBST20 and PBS washing. Non-Faradaic EIS spectra was then recorded on washed electrode using PBS (10 mM, pH 7.4) and the obtained data was converted to capacitance values using  $C = -1/\omega Z''$ , where C is the capacitance,  $\omega$  the angular frequency and  $Z''$  the imaginary part of the impedance. From the capacitance curves (Figure 5b), values were noted at 3 Hz, where a maximum in phase angle is observed (Figure 5a), corresponding to a maximum capacitive effect. The values were then plotted for different concentrations of Her4 for calibration curve (Figure 5c). It is clear from Figure 5c that the capacitance decreases linearly in a log scale with increasing Her4 concentration, which can be attributed to the binding of Her4 proteins to surface bound Affimer. Furthermore, such decrease in capacitance after Her4 binding may be attributed to variations in charge distribution, surface dielectric properties or local conductance via water molecules displacement and ions movement away from the surface during Her4 interaction with surface bound Affimer molecules (Arya et al. 2018; Berggren et al. 2001; Luo and Davis 2013). The electrodes can thus be used for Her4 sensing in the 1 pM to 100 nM range and can be characterised using the relationship for the change in capacitance  $-\Delta C (\mu\text{F}) = 0.07 + 0.03 \log C_{\text{Her4}}$  ( $C_{\text{Her4}}$  is the concentration of Her4 in pM). The Affimer sensor thus exhibits a sensitivity of 0.03  $\mu\text{F}/\log C_{\text{Her4}}$  with a correlation coefficient of 0.996 and a limit of detection lower than 1 pM. For relative changes, results of different electrodes were found to fall within a 4% error range as indicated by error bars in Figure 5c.

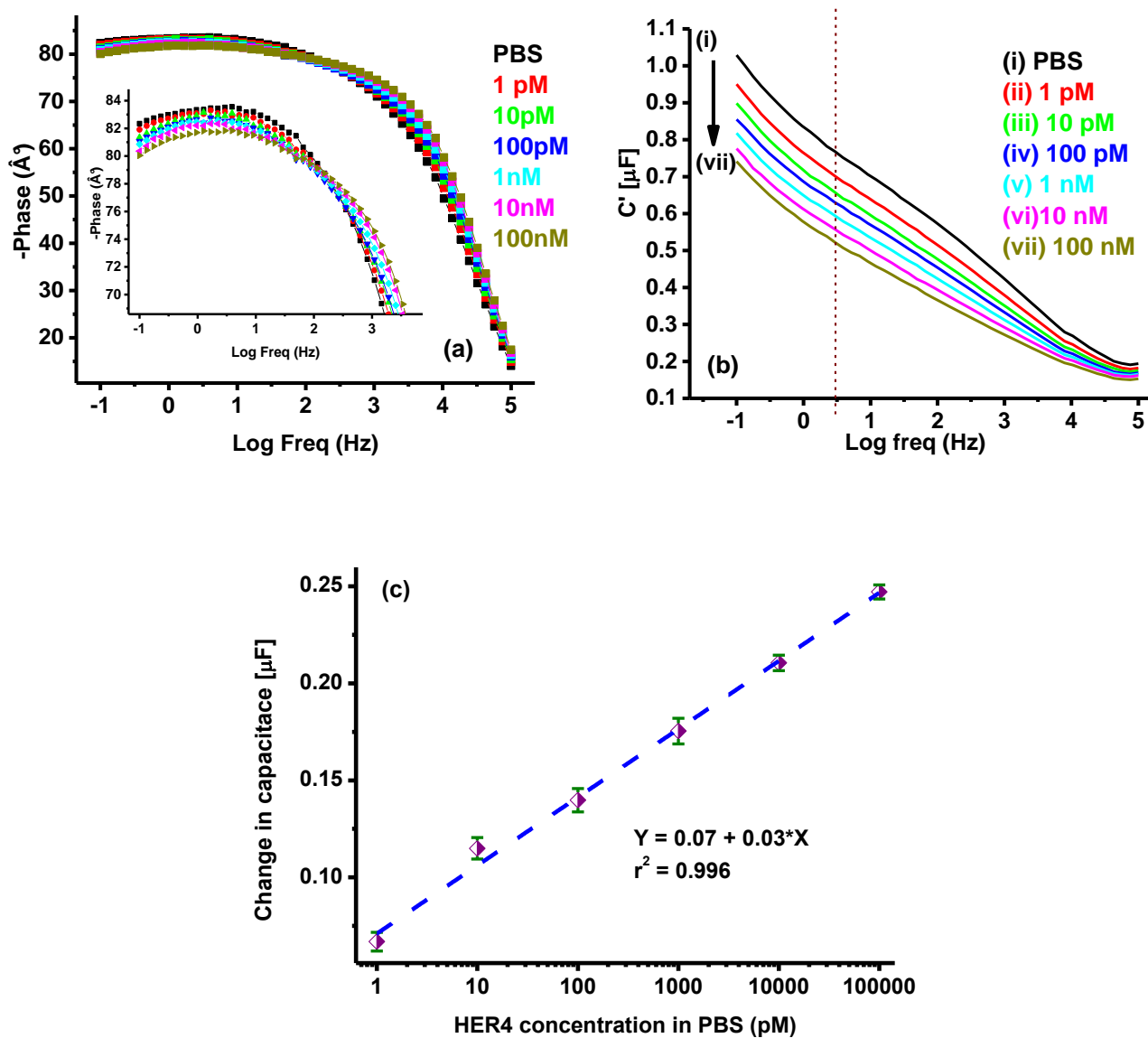
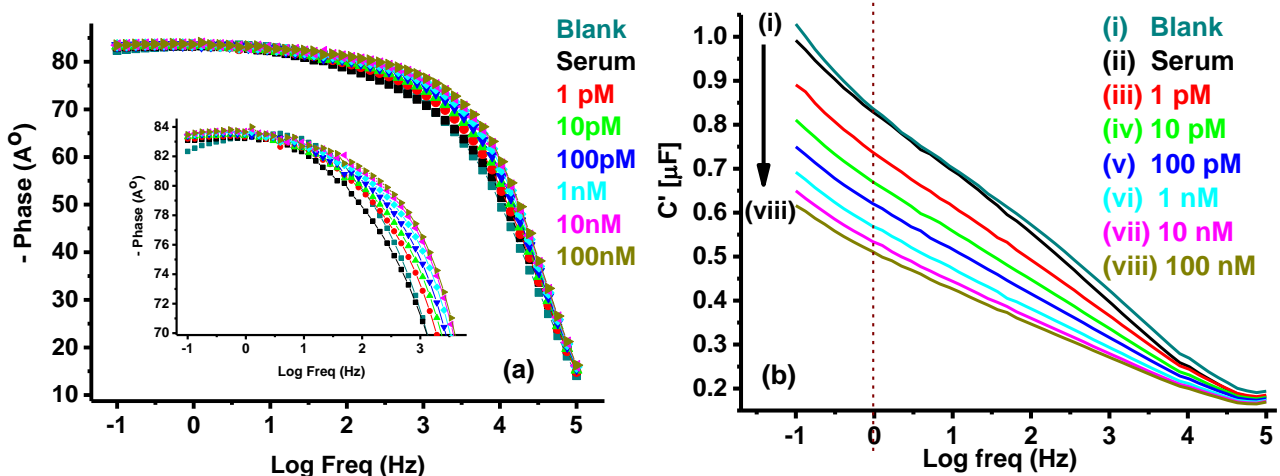


**Figure 5.** (a) EIS phase angle vs. frequency; (b) capacitance data for interaction between surface bound Affimer with Her4 concentrations in PBS; (c) calibration curve using capacitance data for different concentrations at 3 Hz.

### 3.2.2 Capacitive measurement via electrochemical impedance for Her4 in undiluted serum

To validate the electrode for real clinical applications, Affimer sensor electrodes were tested with undiluted serum spiked with Her4 to investigate the interaction between surface bound Affimer and Her4 molecules (1 pM to 100 nM) in presence of all types of serum proteins (Figure 6). Bioassay and measurements were carried out in same manner as done for PBS. Similarly, non-Faradaic EIS data was converted to capacitance and using capacitance curves (Figure 6b);

capacitance values were noted at 1 Hz, where the maximum phase angle is observed (Figure 6a inset). The slight shift in the frequency for which a maximum phase occurs may be attributed to the presence of different types of serum proteins and to different conductivity and ionic strength of the serum compared to PBS. The capacitance values were then plotted for different concentrations of Her4 for the calibration curve presented in Figure 6c. It is clear from Figure 6b that undiluted serum in absence of Her4 shows negligible effects at 1 Hz and a decrease in capacitance was observed only in the presence of Her4 in serum, indicating selective and successful interaction between Her4 proteins and surface bound Affimer. Again, for sensing application, the relative change in capacitance data was estimated and utilised for more significant information. It is clear from Figure 6c that the capacitance decreases linearly in a log scale with increasing Her4 concentration in serum, which can be attributed to the binding of Her4 proteins to surface bound Affimer. Figure 6c shows that the electrodes can be used for Her4 sensing in the 1 pM to 100 nM range following the relationship  $-\Delta C (\mu\text{F}) = 0.095 + 0.049 \log C_{\text{Her4}} (\text{pM})$ . Affimer sensor electrodes thus exhibit a sensitivity of  $0.049 \mu\text{F}/\log C_{\text{Her4}}$  with a correlation coefficient of 0.978 and a limit of detection below 1 pM. Results for different electrodes were found to fall within a 5% error range as indicated by the error bars in Figure 6c.



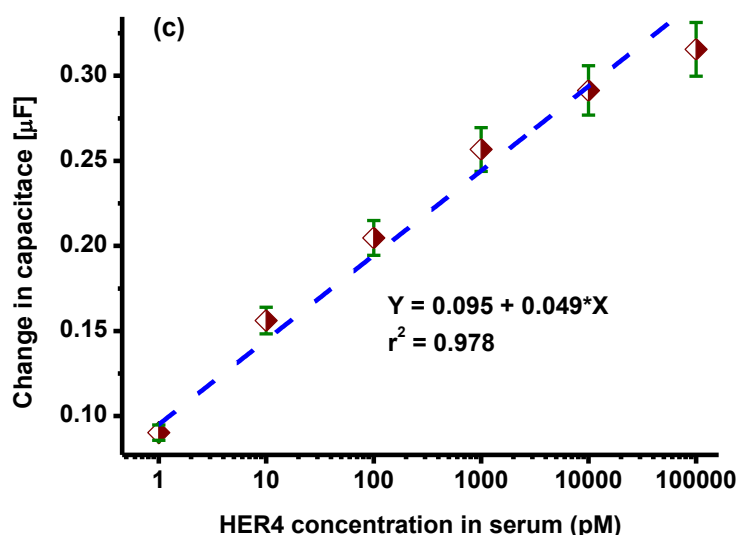


**Figure 6.** (a) EIS phase angle vs. frequency; (b) capacitance data for interaction between surface bound Affimer with Her4 concentrations in undiluted serum; (c) calibration curve using capacitance data for different concentration at 1 Hz.

Comparison of Figure 5 and 6 reveals that the background signal (in the absence of Her4) is similar, suggesting no or negligible non-specific binding of serum proteins to the Affimer sensor. However; for any given concentration of Her4, the signal for Her4 (change in capacitance from blank value) was found to be larger in serum than in buffer (compare Figure 5 and 6). The change in capacitance may be attributed to specific binding effect of the Her4 and exact reason for larger change during measurement in serum is not clear at present, however it may be attributed to one or more potential explanations. First, this increase might be attributed to a better folding of Her4 in serum than in buffer, leading to more productive interactions between molecules of Her4 and the Affimer. A similar effect has also been observed by Park et al. (2002) for measuring Nicotinamide phosphoribosyl transferase via aptamer-based capacitive sensing. Second, the increase could be due to the effect of proteins bound to Her4 that are recruited to the surface through the interaction of Her4 with the Affimer. Further, the slight deviation from linearity for the measurements in the presence of serum may also be attributed to the second explanations. Affimer sensor electrodes were also tested for serum spiked with the control proteins prostate specific antigen and thrombin

and found to result in insignificant effect on signal, suggesting specificity of sensor and again consistent with the idea that the increased signals for Her4 measured in serum compared to buffer is due to specific effects of Her4 and/or Her4-associated serum proteins with the Affimer sensor.

#### **4. Conclusions**

In conclusion, a new Affimer-based alternative strategy has been demonstrated for the detection of Her4 protein biomarker in undiluted serum. The Affimer-based sensor shows slightly better sensitivity as compared to antibody-based assays available commercially (LifeSpan BioSciences) but with a much larger dynamic range (1-70 pM for the ELISA kit), faster response time, ease of use and lower cost. The Affimer sensor also showed excellent selectivity when challenged with other serum protein. The prepared electrodes showed high sensitivity of  $0.049 \mu\text{F}/\log C_{\text{Her4}}$  in undiluted serum with a detection limit lower than 1 pM. The biosensor shows good selective measurement of Her4 in undiluted serum in concentration range of 1pM – 100 nM, with very low non-specific response to serum proteins.

To date only a handful of reports in the literature have described the detection of Her4 in serum so it is as yet unknown whether serum-resident Her4 represents a useful biomarker in cancer or other diseases. However, the Affimer sensor, with its low background and broad linear response range, will enable progress in this field. Furthermore, the fabrication method is simple and can be applied for the detection of other biomarkers in serum samples, paving the way to new platforms for alternative low cost and rapid multiplexed biosensors.

#### **Acknowledgements**

P.Z and P.J were funded by the European Commission FP7 Programme through the Marie Curie Initial Training Network PROSENSE (grant no. 317420, 2012-2016). S.K.A. was funded by the European Commission Horizon 2020 Programme through a Marie Skłodowska-Curie Individual Fellowship (grant no. 655176, 2015-2017).

## References

- Arrata, I.; Barnard, A.; Tomlinson, D.C.; Wilson, A.J. Interfacing native and non-native peptides: using Affimers to recognise  $\alpha$ -helix mimicking foldamers. *Chem. Commun.* **2017**, 53(19), 2834-2837.
- Arya, S.K.; Bhansali, S. Anti-prostate specific antigen (anti-PSA) modified interdigitated microelectrode-based impedimetric biosensor for PSA detection. *Biosens. J.* **2012**, 1, H110601.
- Arya, S.K.; Kongsuphol, P.; Wong, C.C.; Polla, L.J.; Park, M.K. Label free biosensor for sensitive human influenza virus hemagglutinin specific antibody detection using coiled-coil peptide modified microelectrode array based platform. *Sens. Actuators B* **2014**, 194, 127-133.
- Arya, S.K.; Zhuravski, P.; Jolly, P.; Batistuti, M.R.; Mulato, M.; Estrela, P. Capacitive aptasensor based on interdigitated electrode for breast cancer detection in undiluted human serum. *Biosens. Bioelectron.* **2018**, 102, 106-112.
- Bedford, R.; Tiede, C.; Hughes, R.; Curd, A.; McPherson, M.J.; Peckham, M.; Tomlinson, D.C. Alternative reagents to antibodies in imaging applications. *Biophys. Rev.* **2017**, 9(4), 299-308.
- Berggren, C.; Bjarnason, B.; Johansson, G. Capacitive biosensors. *Electroanalysis* **2001**, 13(3), 173-180.
- Bonanno, L.M.; DeLouise, L.A.. Steric crowding effects on target detection in an affinity biosensor. *Langmuir* **2007**, 23(10), 5817-5823.
- Bryan, T.; Luo, X.; Bueno, P.R.; Davis, J.J. An optimised electrochemical biosensor for the label-free detection of C-reactive protein in blood. *Biosens. Bioelectron.* **2013**, 39(1), 94-98.
- Estrela, P.; Paul, D.; Song, Q.; Stadler, L.K.J.; Wang, L.; Huq, E.; Davis, J.J.; Ko Ferrigno, P.; Migliorato, P. Label-free sub-picomolar protein detection with field-effect transistors. *Anal. Chem.* **2010**, 82(9), 3531-3536.

- Gong, Q.; Wang, Y.; Yang, H. A sensitive impedimetric DNA biosensor for the determination of the HIV gene based on graphene-Nafion composite film. *Biosens. Bioelectron.* **2017**, 89(1), 565-569.
- Guan, J.-G.; Miao, Y.-Q.; Zhang, Q.-J. Impedimetric biosensors. *J. Biosci. Bioeng.* 2004, 97(4), 219-226.
- Hollmén, M.; Liu, P.; Kurppa, K.; Wildiers, H.; Reinvall, I.; Vandorpe, T.; Smeets, A.; Deraedt, K.; Vahlberg, T.; Joensuu, H.; Leahy, D.J.; Schöffski, P. Elenius, K. Proteolytic processing of ErbB4 in breast cancer. *PLoS One* **2012**, 7(6), e39413.
- Johnson, A.; Song, Q.; Ko Ferrigno, P.; Bueno, P.R.; Davis, J.J. Sensitive Affimer and antibody based impedimetric label-free assays for C-reactive protein. *Anal. Chem.* **2012**, 84(15), 6553-6560.
- Katz, E.; Willner, I. Probing biomolecular interactions at conductive and semiconductive surfaces by impedance spectroscopy: routes to impedimetric immunosensors, DNA-sensors, and enzyme biosensors. *Electroanalysis* **2003**, 15(11), 913-947.
- Keum, J.-W.; Bermudez, H. Enhanced resistance of DNA nanostructures to enzymatic digestion. *Chem. Commun.* **2009**, (45), 7036-7038.
- Ko Ferrigno, P. Non-antibody protein-based biosensors. *Essays Biochem.* **2016**, 60(1), 19-25.
- Koutsoumpeli, E.; Tiede, C.; Murray, J.; Tang, A.; Bon, R.S.; Tomlinson, D.C.; Johnson, S. Antibody mimetics for the detection of small organic compounds using a quartz crystal microbalance. *Anal. Chem.* **2017**, 89(5), 3051-3058.
- Kyle, H.F.; Wickson, K.F.; Stott, J.; Burslem, G.M.; Breeze, A.L.; Tiede, C.; Tomlinson, D.C.; Warriner, S.L.; Nelson, A.; Wilson, A.J.; Edwards, T.A. Exploration of the HIF-1 $\alpha$ /p300 interface using peptide and Adhiron phage display technologies. *Mol. BioSyst.* **2015**, 11(10), 2738-2749.
- Luo, X.; Davis, J.J. Electrical biosensors and the label free detection of protein disease biomarkers. *Chem. Soc. Rev.* **2013**, 42(13), 5944-5962.

- Miodek, A.; Regan, E.; Bhalla, N.; Hopkins, N.; Goodchild, S.; Estrela, P. Optimisation and characterisation of anti-fouling ternary SAM layers for impedance-based aptasensors. *Sensors* **2015**, 15(10), 25015.
- Mucciarini, C.; Rossi, G.; Bertolini, F.; Valli, R.; Cirilli, C.; Rashid, I.; Marcheselli, L.; Luppi, G.; Federico, M. Incidence and clinicopathologic features of gastrointestinal stromal tumors: a population-based study. *BMC Cancer* **2007**, 7, 230.
- Nilsson, B.; Bümming, P.; Meis-Kindblom, J.M.; Odén, A.; Dortok, A.; Gustavsson, B.; Sablinska, K.; Kindblom, L.G. Gastrointestinal stromal tumors: the incidence, prevalence, clinical course, and prognostication in the preimatinib mesylate era: a population-based study in Western Sweden. *Cancer* **2005**, 103(4), 821-829.
- Olsen, D.A.; Østergaard, B.; Bokmand, S.; Wamberg, P.A.; Jakobsen, E.H.; Jakobsen, A.; Brandslund, I. HER1-4 protein concentrations in normal breast tissue from breast cancer patients are expressed by the same profile as in the malignant tissue. *Clin. Chem. Lab. Med.* **2009**, 47(8), 977-984.
- Park, J.W.; Saravan Kallempudi, S.; Niazi, J.H.; Gurbuz, Y.; Youn, B.-S.; Gu, M.B. Rapid and sensitive detection of Nampt (PBEF/visfatin) in human serum using an ssDNA aptamer-based capacitive biosensor. *Biosens. Bioelectron.* **2012**, 38(1), 233-238.
- Pasha, S.K.; Kaushik, A.; Vasudev, A.; Snipes, S.A.; Bhansali, S. Electrochemical immunosensing of saliva cortisol. *J. Electrochem. Soc.* **2014**, 161(2), B3077-B3082.
- Pui, T.S.; Kongsuphol, P.; Arya, S.K.; Bansal, T. Detection of tumor necrosis factor (TNF- $\alpha$ ) in cell culture medium with label free electrochemical impedance spectroscopy. *Sens. Actuators B* **2013**, 181, 494-500.
- Qureshi, A.; Gurbuz, Y.; Niazi, J.H. Label-free detection of cardiac biomarker using aptamer based capacitive biosensor. *Proc. Eng.* **2010**, 5, 828-830.

- Raina, M.; Sharma, R.; Deacon, S.E.; Tiede, C.; Tomlinson, D.; Davies, A.G.; McPherson, M.J.; Wälti, C. Antibody mimetic receptor proteins for label-free biosensors. *Analyst* **2015**, 140(3), 803-810.
- Ramón-Azcón, J.; Valera, E.; Rodríguez, Á.; Barranco, A.; Alfaro, B.; Sanchez-Baeza, F.; Marco, M.P. An impedimetric immunosensor based on interdigitated microelectrodes (ID $\mu$ E) for the determination of atrazine residues in food samples. *Biosens. Bioelectron.* **2008**, 23(9), 1367-1373.
- Rawlings, A.E.; Bramble, J.P.; Tang, A.A.S.; Somner, L.A.; Monnington, A.E.; Cooke, D.J.; McPherson, M.J.; Tomlinson, D.C.; Staniland, S.S. Phage display selected magnetite interacting Adhirons for shape controlled nanoparticle synthesis. *Chem. Sci.* **2015**, 6(10), 5586-5594.
- Rimmele, M. Nucleic acid aptamers as tools and drugs: recent developments. *ChemBioChem* **2003**, 4(10), 963-971.
- Sandvik, O.M.; Søreide, K.; Kvaløy, J.T.; Gudlaugsson, E.; Søreide, J.A. Epidemiology of gastrointestinal stromal tumours: Single-institution experience and clinical presentation over three decades. *Cancer Epidemiol.* **2011**, 35(6), 515-520.
- Santos, A.; Davis, J.J.; Bueno, P.R. Fundamentals and applications of impedimetric and redox capacitive biosensors. *J. Anal. Bioanal. Tech.* **2014**, S7:016.
- Sharma, R.; Deacon, S.E.; Nowak, D.; George, S.E.; Szymonik, M.P.; Tang, A.A.S.; Tomlinson, D.C.; Davies, A.G.; McPherson, M.J.; Wälti, C. Label-free electrochemical impedance biosensor to detect human interleukin-8 in serum with sub-pg/ml sensitivity. *Biosens. Bioelectron.* **2016**, 80, 607-613.
- Song, S.; Wang, L.; Li, J.; Fan, C.; Zhao, J. Aptamer-based biosensors. *Trends Anal. Chem.* **2008**, 27(2), 108-117.
- Steigen, S.E.; Eide, T.J. Gastrointestinal stromal tumors (GISTs): a review. *APMIS* **2009**, 117(2), 73-86.

Straw, S.; Ko Ferrigno, P.; Song, Q.; Tomlinson, D.; Del Galdo, F. Proof of concept study to identify candidate biomarkers of fibrosis using high throughput peptide aptamer microarray and validate by enzyme linked immunosorbant assay. *J. Biomed. Sci. Eng.* **2013**, 6(8B), 32-42.

Sylvia, P.; Brehm, S.O.; Hoch, H.J.A. DNA-binding proteins in human serum. *Biochem. Biophys. Res. Commun.* **1975**, 63(1), 24-31.

Tebbutt, N.; Pedersen, M.W.; Johns, T.G. Targeting the ERBB family in cancer: couples therapy. *Nat. Rev. Cancer* **2013**, 13(9), 663-673.

Tiede, C.; Tang, A.A.S.; Deacon, S.E.; Mandal, U.; Nettleship, J.E.; Owen, R.L.; George, S.E.; Harrison, D.J.; Owens, R.J.; Tomlinson, D.C.; McPherson, M.J. Adhiron: a stable and versatile peptide display scaffold for molecular recognition applications. *Protein Eng. Des. Sel.* **2014**, 27(5), 145-155.

Tiede, C.; Bedford, R.; Heseltine, S.J.; Smith, G.; Wijetunga, I.; Ross, R.; AlQallaf, D.; Roberts, A.P.E.; Balls, A.; Curd, A.; Hughes, R.E.; Martin, H.; Needham, S.R.; Zanetti-Domingues, L.C.; Sadigh, Y.; Peacock, T.P.; Tang, A.A.; Gibson, N.; Kyle, H.; Platt, G.W.; Ingram, N.; Taylor, T.; Coletta, L.P.; Manfield, I.; Knowles, M.; Bell, S.; Esteves, F.; Maqbool, A.; Prasad, R.K.; Drinkhill, M.; Bon, R.S.; Patel, V.; Goodchild, S.A.; Martin-Fernandez, M.; Owens, R.J.; Nettleship, J.E.; Webb, M.E.; Harrison, M.; Lippiat, J.D.; Ponnambalam, S.; Peckham, M.; Smith, A.; Ko Ferrigno, P.; Johnson, M.; McPherson, M.J.; Tomlinson, D.C. Affimer proteins are versatile and renewable affinity reagents. *eLife* **2017**, 6, e24903.

Varshney, M.; Li, Y. Interdigitated array microelectrodes based impedance biosensors for detection of bacterial cells. *Biosens. Bioelectron.* **2009**, 24(10), 2951-2960.

Vasudev, A.; Kaushik, A.; Bhansali, S. Electrochemical immunosensor for label free epidermal growth factor receptor (EGFR) detection. *Biosens. Bioelectron.* **2013**, 39(1), 300-305.

Vazquez-Lombardi, R.; Phan, T.G.; Zimmermann, C.; Lowe, D.; Jermutus, L.; Christ, D. Challenges and opportunities for non-antibody scaffold drugs. *Drug Discov. Today* **2015**, 20(10), 1271-1283.

- Wang, R.; Wang, Y.; Lassiter, K.; Li, Y.; Hargis, B.; Tung, S.; Berghman, L.; Bottje, W. Interdigitated array microelectrode based impedance immunosensor for detection of avian influenza virus H5N1. *Talanta* **2009**, 79(2), 159-164.
- Wang, B.; Jing, R.; Qi, H.; Gao, Q.; Zhang, C. Label-free electrochemical impedance peptide-based biosensor for the detection of cardiac troponin I incorporating gold nanoparticles modified carbon electrode. *J. Electroanal. Chem.* **2016**, 781, 212-217.
- Wang, S.X.; Acha, D.; Shah, A.J.; Hills, F.; Roitt, I.; Demosthenous, A.; Bayford, R.H. Detection of the tau protein in human serum by a sensitive four-electrode electrochemical biosensor. *Biosens. Bioelectron.* **2017**, 92, 482-488.
- Woodman, R.; Yeh, J.T.H.; Laurenson, S.; Ko Ferrigno, P. Design and validation of a neutral protein scaffold for the presentation of peptide aptamers. *J. Mol. Biol.* **2005**, 352(5), 1118-1133.
- Xu, Y.; Cheng, G.; He, P.; Fang, Y. A review: electrochemical aptasensors with various detection strategies. *Electroanalysis* **2009**, 21(11), 1251-1259.
- Xu, M.; Luo, X.; Davis, J.J. The label free picomolar detection of insulin in blood serum. *Biosens. Bioelectron.* **2013**, 39(1), 21-25.
- Zhao, W.Y.; Zhuang, C.; Xu, J.; Wang, M.; Zhang, Z.Z.; Tu, L.; Wang, C.J.; Ling, T.L.; Cao, H.; Zhang, Z.G. HER4 is a novel prognostic biomarker in gastrointestinal stromal tumor specifically originated from stomach. *Am. J. Cancer Res.* **2014**, 4(6), 838-849.

TOC Figure

